Chemical Physics 493 (2017) 194–199

Contents lists available at ScienceDirect

Chemical Physics

journal homepage: www.elsevier.com/locate/chemphys

Plasmon enhanced heterogeneous electron transfer with continuous band energy model

Dandan Zhao, Lu Niu, Luxia Wang *

Department of Physics, University of Science and Technology Beijing, 100083 Beijing, China

ARTICLE INFO

Article history:
Received 16 May 2017
In final form 15 July 2017
Available online 17 July 2017

Keywords:
Metal nanoparticle
Density matrix theory
Plasmon enhancement

ABSTRACT

Photoinduced charge injection from a perylene dye molecule into the conduction band of a TiO_2 system decorated by a metal nanoparticles (MNP) is studied theoretically. Utilizing the density matrix theory the charge transfer dynamics is analyzed. The continuous behavior of the TiO_2 conduction band is accounted for by a Legendre polynomials expansion. The simulations consider optical excitation of the dye molecule coupled to the MNP and the subsequent electron injection into the TiO_2 semiconductor. Due to the energy transfer coupling between the molecule and the MNP optical excitation and subsequent charge injection into semiconductor is strongly enhanced. The respective enhancement factor can reach values larger than 10^3. Effects of pulse duration, coupling strength and energetic resonances are also analyzed. The whole approach offers an efficient way to increase charge injection in dye-sensitized solar cells.

© 2017 Published by Elsevier B.V.

1. Introduction

The dye molecule connected with the semiconductor material (such as TiO_2) with a porous structure through an anchor molecule is the main part of the dye-sensitized solar cell [1]. There is an ongoing interest in theoretical and experimental studies on improving the efficiency of charge transfer from the molecule to semiconductor.

A lot of evidences exist that surface plasmons of metal nanoparticles (MNPs) can greatly improve the efficiency of a solar cell [2]. Driven by an external field, the free electrons in the conduction band of MNP show collective oscillations known as the surface plasmon. In the resonance state, the energy of the external field is effectively converted to the plasmons. By means of the coupling to the dye molecule, the energy is further transferred to the dye molecule. MNP-molecule coupling have various forms, such as multi-layer structure model [3], core-shell nanoparticle model [4], nanocomposite films containing metal nanoparticles and molecules [5] and so on. There were numerous attempts described in literatures to achieve MNP induced efficiency enhancement of the dye-sensitized solar cell. Such as metal nano-structures combined with thin-film solar cells [6], photosensitization of bulk TiO_2 by embedded MNPs [7], TiO_2-nanostructures decorated with MNPs [8,9] and so on.

Currently, there are applications that employ metal nanoparticle plasmon resonance, for example, in the polymer solar cells [10–12], the devices with nanorod structures and sputtered metallic nanoparticles [13,14]. Irradiating metal nanoparticles with light at their plasmon frequency generates intense electric fields at the surface of the nanoparticle. The frequency of this resonance can be tuned by varying the nanoparticle size, shape [15], material, and proximity to other nanoparticles. We also have theoretical attempts on the enhancement effect of MNP [16,17], with the tight-binding model describing the TiO_2 semiconductor. The shortcoming of that is the wavefunction reflection on the boundary of the semiconductor, which strongly restricts us to calculate the bulk scale TiO_2 cluster and that requires more computational resources. Continuous band model of semiconductor used in Refs. [18,19] can effectively describe the quasi-continuous energy level of TiO_2, which introduced the Legendre polynomials expansion. We also note that the mirror charge effect can be ignored during the charge injection into the semiconductor [16]. Still, a two electronic level model [20,21] is used for dye molecule. The description of the dye-MNP system could be carried out on the basis of the inclusion of that part of the Coulomb coupling, which is responsible for excitation energy exchange [22]. Such a uniform description accounts for local field induced molecular absorption enhancement as well as for molecular excitation energy quenching [16]. Fig. 1 shows the energy level arrangement of the MNP decorated molecule-semiconductor system.

The paper is organized as follows. In the subsequent section we introduce the used model of the dye molecule TiO_2-semiconductor

* Corresponding author.
E-mail address: luxiawang@sas.ustb.edu.cn (L. Wang).

http://dx.doi.org/10.1016/j.chemphys.2017.07.005
0301-0104/© 2017 Published by Elsevier B.V.

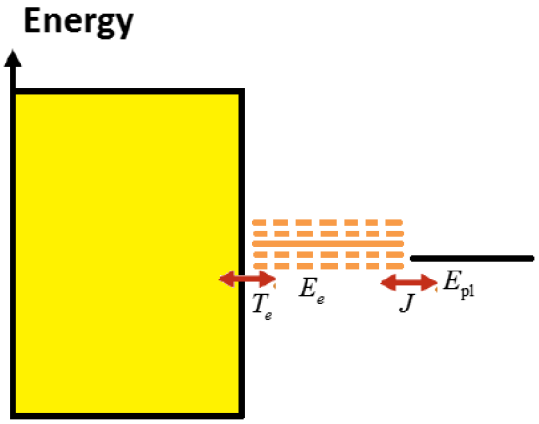

Fig. 1. Energy level arrangement displaying the energies which constitute the Hamiltonian, Eq. (1). The left rectangle symbolizes the energy band of the TiO_2. The molecular excited state with energy E_e (shown the orange lines) is coupled to the MNP dipole plasmon state with E_{pl} (shown the short black solid line) via the coupling J. Charge injection to the semiconductor conduction band is realized by the transfer coupling T_e. (For interpretation of the references to colour in this figure caption, the reader is referred to the web version of this article.)

decorated by one MNP and the density matrix theory of charge injection. In Section 3 we present the results and corresponding discussions. Some concluding remarks are presented in Section 4.

2. Model and theory

The dye molecule, semiconductor, MNP system is treated as described in [16–18]. Therefore, an expansion is carried out with respect to system product states [17]. The ground-state φ_g does not contribute since the respective energy has been set equal to zero, cf. the energy sketch in Fig. 1. The remaining Hamiltonian reads

$$H(t) = H_{\text{mol}} + H_{\text{sem}} + H_{\text{mnp}} + H_{\text{mol-sem}} + H_{\text{mol-mnp}} + H_{\text{field}}(t). \quad (1)$$

The Hamiltonian of the excited dye molecule is

$$H_{\text{mol}} = \hbar\varepsilon_e |\varphi_e\rangle\langle\varphi_e|, \quad (2)$$

where $\hbar\varepsilon_e$ is the molecular electronic excitation energy (at the nuclear equilibrium configuration) and φ_e represents the product of the excited molecular state, the MNP ground-state and the empty semiconductor conduction band state.

The semiconductor conduction-band Hamiltonian takes the form [16]

$$H_{\text{sem}} = \sum_{\mathbf{k}} \hbar\varepsilon_{\mathbf{k}} |\varphi_{\mathbf{k}}\rangle\langle\varphi_{\mathbf{k}}|, \quad (3)$$

with $\mathbf{k}$ as the quasi-wave vector. The $\hbar\varepsilon_{\mathbf{k}}$ are the conduction band energies (including the energy necessary to remove the electron from the dye and put it into the TiO_2 lattice; cf. [17]). For further discussion, we write $\hbar\varepsilon_{\mathbf{k}}$ as $E_c + \hbar\omega_{\mathbf{k}}$, with the lower band-edge E_c and with $\hbar\omega_{\mathbf{k}}$ running over the conduction band. $\varphi_{\mathbf{k}}$ denotes the product states which include the electron in the semicondcutor, the cationic dye state, and again the MNP ground-state.

The Hamiltonian of the excited MNP has the form [17]

$$H_{\text{mnp}} = \sum_{I} \hbar\varepsilon_I |\varphi_I\rangle\langle\varphi_I|, \quad (4)$$

with the dipole plasmon energy $E_{\text{pl}} = \hbar\varepsilon_I$. I counts the three degenerated dipole plasmon ($I = x, y, z$ indicates excitations in the three directions of a Cartesian coordinate system). The state φ_I covers the excited MNP state, the dye molecule ground-state and the state referring to the empty TiO_2 conduction band.

The molecule-MNP coupling Hamiltonian is written as

$$H_{\text{mol-mnp}} = \sum_{I} J_{Ie} |\varphi_I\rangle\langle\varphi_e| + H.c., \quad (5)$$

and the coupling matrix element J_{Ie} can be approximated as an interaction between molecular and MNP transition dipole moments. Such an interaction of the excitation energy transfer type is of minor importance between the MNP and the TiO_2 system since interband transitions of the latter lie in the UV.

The Hamiltonian of the molecule-semiconductor interaction reads [18]

$$H_{\text{mol-sem}} = \sum_{\mathbf{k}} T_{\mathbf{k}e} |\varphi_{\mathbf{k}}\rangle\langle\varphi_e| + H.c., \quad (6)$$

where charge injection from $|\varphi_e\rangle$ into the manifold of states $|\varphi_{\mathbf{k}}\rangle$ is realized by the transfer coupling $T_{\mathbf{k}e}$.

The Hamiltonian of interaction between the system and external applied laser field takes the form [16]

$$H_{\text{field}}(t) = -\boldsymbol{E}(t)\cdot\hat{\boldsymbol{\mu}} = -\boldsymbol{E}(t)\cdot\left(\boldsymbol{d}_{\text{eg}}|\varphi_e\rangle\langle\varphi_g| + \sum_I \boldsymbol{d}_{I0}|\varphi_I\rangle\langle\varphi_g| + H.c.\right), \quad (7)$$

where $\boldsymbol{d}_{\text{eg}}$ and $\boldsymbol{d}_{I0}$ are dipole moments of molecule and plasmons respectively, they have the form of $\boldsymbol{d}_{\text{eg}} = d_{\text{eg}}\boldsymbol{e}_z$ and $\boldsymbol{d}_{I0} = d_{\text{pl}}\boldsymbol{e}_I$, $\boldsymbol{E}(t)$ is the time-dependent electric field strength of a pulsed optical excitation with the following form

$$\boldsymbol{E}(t) = \boldsymbol{e}E(t)\exp(-i\omega_0 t) + \text{c.c.}, \quad (8)$$

here, $\boldsymbol{e}$ is the unit vector of field polarization (here we set that the direction of $\boldsymbol{e}$ is consistent with that of $\boldsymbol{d}_{\text{eg}}$) and ω_0 is the carrier frequency. The envelope $E(t)$ has the Gaussian shape

$$E(t) = E_0\exp(-2(t-t_p)^2/\tau_p^2), \quad (9)$$

with amplitude E_0, pulse center at t_p and duration τ_p. All the used parameters can be found in Table 1 (for motivation see also our earlier work of Refs. [16–19]).

The injection process is described in the framework of open system dynamics with density matrix theory, and the related density matrix reads

$$\rho_{\alpha\beta}(t) = \langle\varphi_\alpha|\hat{\rho}(t)|\varphi_\beta\rangle, \quad (10)$$

where α and β label the different states introduced beforehand, $\hat{\rho}$ is the reduced density operator. To account for energy relaxation and dephasing an application of the standard quantum master equation is appropriate. Due to fast plasmon decay we may take a version where the dissipative part of the equations does not couple populations and coherences [16]

$$\frac{\partial}{\partial t}\rho_{\alpha\beta}(t) = -i\tilde{\omega}_{\alpha\beta}\rho_{\alpha\beta}(t) - \frac{i}{\hbar}\sum_\gamma(\upsilon_{\alpha\gamma}\rho_{\gamma\beta}(t) - \upsilon_{\gamma\beta}\rho_{\alpha\gamma}(t)) - \delta_{\alpha,\beta}\sum_\gamma(k_{\alpha\to\gamma}\rho_{\alpha\alpha}(t) - k_{\gamma\to\alpha}\rho_{\gamma\gamma}(t)), \quad (11)$$

Table 1
Parameters introduced in Refs. [16–19] and used here (for explanation see text).

d_{eg}	3 D
d_{pl}	2925 D
$\hbar\gamma_{\text{mol}}$	3 meV
$\hbar\gamma_{\text{pl}}$	28.6 meV
r_{mnp}	10 nm
$\hbar\Delta\omega$	3 eV
$\tau_p(t_p)$	10 fs (15 fs)
E_0	5×10^5 V/m
$\hbar\varepsilon_e$	2.6 eV, 2.4–2.9 eV
$\hbar\omega_I$	2.6 eV
$\hbar\omega_0$	2.6 eV, 2.4–2.9 eV

where the complex transition frequencies $\widetilde{\omega}_{\alpha\beta} = \omega_{\alpha\beta} - i(1-\delta_{\alpha\beta})r_{\alpha\beta}$, with $\omega_{\alpha\beta} = \varepsilon_\alpha - \varepsilon_\beta$ and the $r_{\alpha\beta}$ are the dephasing rate. The coupling matrix $\hbar v_{\alpha\beta}$ covers all electron transfer matrix elements $T_{\mathbf{ke}}$, the molecule-MNP energy transfer coupling J_{Ie} and the coupling to the time-dependent external field via $-\boldsymbol{d}_{\mathrm{eg}}\cdot\boldsymbol{E}(t)$ and $-\boldsymbol{d}_{I0}\cdot\boldsymbol{E}(t)$. The transition rates $k_{\alpha\to\beta}$ determine the dephasing rate $r_{\alpha\beta}$ according to the standard formula $1/2\sum_\gamma(k_{\alpha\to\gamma}+k_{\beta\to\gamma})$. Here, the rate only covers the contribution due to plasmon decay. Molecular decay does not play any role in the time region studied here (molecular dephasing, however, is considered). Accordingly, we have $k_{I\to g} = 2\gamma_{\mathrm{pl}}$ [16]. The used version of the quantum master equation is sufficient when removing very fast oscillations by carrying out the rotating wave approximation (see below).

For the following it is useful to change the **k** dependence of the band energy and the transfer coupling to a continuous frequency dependence. This becomes possible by introducing the density of state (DOS) [18]

$$N(\omega) = \sum_{\mathbf{k}}\delta(\omega-\varepsilon_{\mathbf{k}}). \tag{12}$$

The density matrix $\rho_{\mathbf{kk}'}$ is rewritten as a function of two continuous frequency according to

$$\rho(\omega,\omega') = \sum_{\mathbf{kk}'}\delta(\omega-\varepsilon_{\mathbf{k}})\delta(\omega'-\varepsilon_{\mathbf{k}'})\rho_{\mathbf{kk}'}. \tag{13}$$

In addition, the type $\rho_{\mathrm{e}\mathbf{k}}, \rho_{\mathrm{g}\mathbf{k}}$ and $\rho_{I\mathbf{k}}$ depending on a single **k** quantum number can be written, for example, as

$$\rho_{\mathrm{e}}(\omega) = \sum_{\mathbf{k}}\delta(\omega-\varepsilon_{\mathbf{k}})\rho_{\mathrm{e}\mathbf{k}}. \tag{14}$$

A function $f(\omega)$ of the continuous frequency ω is expanded with respect to $u_r(\omega)$

$$f(\omega) = \sum_r u_r(\omega) f_r, \tag{15}$$

with

$$f_r = \int_0^{\Delta\omega} d\omega f(\omega)u_r(\omega) = \langle f u_r\rangle_\omega, \tag{16}$$

here, $u_r(\omega)$ are orthogonal polynomials substantiated by Legendre polynomials. $\hbar\Delta\omega$ defines the width of the continuous band energies. Furthermore, we have the form

$$\langle\omega f u_r\rangle_\omega = \int_0^{\Delta\omega} d\omega\cdot\omega f(\omega)u_r(\omega), \tag{17}$$

and

$$\rho_{rp}(t) = \int_0^{\Delta\omega} d\omega d\omega' u_r(\omega)\rho(\omega,\omega';t)u_p(\omega') = \langle u_r\rho(t)u_p\rangle_{\omega\omega'}. \tag{18}$$

To account for the external laser pulse excitation in an efficient way, we apply the rotating wave approximation (RWA) and replace $\rho_{\mathrm{eg}}(t)$ by $\exp(-i\omega_0 t)\times r_{\mathrm{eg}}(t), \rho_{Ig}(t)$ by $\exp(-i\omega_0 t)\times r_{Ig}(t)$. Furthermore we set $\rho_{\mathrm{gg}}(t) = r_{\mathrm{gg}}(t), \rho_{\mathrm{ee}}(t) = r_{\mathrm{ee}}(t), \rho^*_{\mathrm{gr}}(t) = r^*_{\mathrm{gr}}(t)e^{i\omega_0 t}, \rho_{eI}(t) = r_{eI}(t), \rho_{II'}(t) = r_{II'}(t), \rho_{\mathrm{ep}}(t) = r_{\mathrm{ep}}(t), \rho_{Ip}(t) = r_{Ip}(t)$ and $\rho_{rp}(t) = r_{rp}(t)$. Vibrational contribution are less significant contrasting with the enhancement effect of MNP. Neglecting all fast oscillating terms, we arrive at following equations:

$$\frac{\partial}{\partial t}r_{\mathrm{gg}} = 2\sum_I\gamma_{\mathrm{pl}}r_{II} + \frac{i}{\hbar}(d^*_{\mathrm{eg}}E^*r_{\mathrm{eg}} - \mathrm{c.c.}) + \frac{i}{\hbar}\sum_I(d^*_{\mathrm{pl}}E^*r_{Ig} - \mathrm{c.c.}), \tag{19}$$

$$\frac{\partial}{\partial t}r_{\mathrm{eg}} = -i(\varepsilon_{\mathrm{e}} - \omega_0 - i\gamma_{\mathrm{mol}})r_{\mathrm{eg}} - \frac{i}{\hbar}\sum_I J_{eI}r_{Ig} - \frac{i}{\hbar}\langle T_{\mathrm{e}}r^*_{\mathrm{g}}\rangle_\omega + \frac{i}{\hbar}d_{\mathrm{eg}}E(r_{\mathrm{gg}} - r_{\mathrm{ee}}) - \frac{i}{\hbar}\sum_I d_{\mathrm{pl}}Er_{eI}, \tag{20}$$

$$\frac{\partial}{\partial t}r_{Ig} = -i(\omega_I - \omega_0 - i\gamma_{\mathrm{pl}})r_{Ig} - \frac{i}{\hbar}J_{Ie}r_{\mathrm{eg}} + \frac{i}{\hbar}d_{\mathrm{pl}}Er_{\mathrm{gg}} - \frac{i}{\hbar}d_{\mathrm{eg}}Er_{Ie} - \frac{i}{\hbar}\sum_{I'}d_{\mathrm{pl}}Er_{II'}, \tag{21}$$

$$\frac{\partial}{\partial t}r_{\mathrm{ee}} = -\frac{i}{\hbar}\sum_I(J_{eI}r_{Ie} - \mathrm{c.c.}) - \frac{i}{\hbar}(\langle T_{\mathrm{e}}r^*_{\mathrm{e}}\rangle_\omega - \mathrm{c.c.}) + \frac{i}{\hbar}(d_{\mathrm{eg}}Er_{\mathrm{ge}} - \mathrm{c.c.}), \tag{22}$$

$$\frac{\partial}{\partial t}r_{eI} = -i(\varepsilon_{\mathrm{e}} - \omega_I - i\gamma_{\mathrm{mol}} - i\gamma_{\mathrm{pl}})r_{eI} - \frac{i}{\hbar}\sum_{I'}J_{eI'}r_{I'I} - \frac{i}{\hbar}\langle T_{\mathrm{e}}r^*_I\rangle_\omega + \frac{i}{\hbar}J_{eI}r_{\mathrm{ee}} + \frac{i}{\hbar}d_{\mathrm{eg}}Er_{gI} - \frac{i}{\hbar}d^*_{\mathrm{pl}}E^*r_{\mathrm{eg}}, \tag{23}$$

$$\frac{\partial}{\partial t}r_{II'} = -2i\gamma_{\mathrm{pl}}r_{II'} - \frac{i}{\hbar}(J_{Ie}r_{eI'} - J_{eI'}r_{Ie}) - \frac{i}{\hbar}d^*_{\mathrm{pl}}E^*r_{Ig} + \frac{i}{\hbar}d_{\mathrm{pl}}Er_{gI'}, \tag{24}$$

$$\frac{\partial}{\partial t}r^*_{\mathrm{gr}} = -i\langle\omega r^*_{\mathrm{g}}u_r\rangle_\omega - \frac{i}{\hbar}\sum_I d_{\mathrm{pl}}Er^*_{Ir} - i(-\omega_0 - i\gamma_{\mathrm{mol}})r^*_{\mathrm{gr}} - \frac{i}{\hbar}d_{\mathrm{eg}}Er^*_{\mathrm{er}} - \frac{i}{\hbar}\langle T^*_{\mathrm{e}}Nu_r\rangle_\omega r_{\mathrm{eg}}, \tag{25}$$

$$\frac{\partial}{\partial t}r_{\mathrm{ep}} = -\frac{i}{\hbar}\sum_I J_{eI}r_{Ip} + i\langle r_{\mathrm{e}}\omega' u_p\rangle_{\omega'} - i(\varepsilon_{\mathrm{e}} - i\gamma_{\mathrm{mol}})r_{\mathrm{ep}} - \frac{i}{\hbar}\times\langle T_{\mathrm{e}}r_p\rangle_\omega + \frac{i}{\hbar}\langle T_{\mathrm{e}}Nu_p\rangle_{\omega'}r_{\mathrm{ee}} + \frac{i}{\hbar}d_{\mathrm{eg}}Er_{gp}, \tag{26}$$

$$\frac{\partial}{\partial t}r_{Ip} = i\langle r_I\omega' u_p\rangle_{\omega'} - \frac{i}{\hbar}J_{Ie}r_{\mathrm{ep}} + \frac{i}{\hbar}d_{\mathrm{pl}}Er_{gp} - i(\omega_I - i\gamma_{\mathrm{pl}})r_{Ip} + \frac{i}{\hbar}\times\langle T_{\mathrm{e}}Nu_p\rangle_{\omega'}r_{Ie}, \tag{27}$$

$$\frac{\partial}{\partial t}r_{rp} = -i\langle u_r\omega r u_p\rangle_{\omega\omega'} + i\langle u_r r\omega' u_p\rangle_{\omega\omega'} - \frac{i}{\hbar}\langle u_r NT_{\mathrm{e}}\rangle_\omega r_{\mathrm{ep}} + \frac{i}{\hbar}\times\langle NT_{\mathrm{e}}u_p\rangle_{\omega'}r^*_{\mathrm{er}}, \tag{28}$$

The population of dye molecular excited state is

$$P_{\mathrm{e}}(t) = r_{\mathrm{ee}}(t), \tag{29}$$

and the population of the excited state of dipole plasmons reads

$$P_{\mathrm{pl}}(t) = \sum_I r_{II}(t), \tag{30}$$

to characterize the process of charge injection in the following we take the total probability

$$P_{\mathrm{sem}}(t) = 1 - P_{\mathrm{e}}(t) - P_{\mathrm{pl}}(t), \tag{31}$$

to have an electron in the TiO_2-band.

To valuate the MNP enhancement effect, we analyze the steady-state probability $P_{\mathrm{sem}}(\tau_{ss})$ with τ_{ss} as the time at which the population reaches its steady state and compute this quantity in the absence of the MNP $P^{(0)}(\tau_{ss})$ and in its presence $P^{(\mathrm{MNP})}(\tau_{ss})$. Then, an enhancement factor can defined as

$$\mathrm{Enh} = P^{(\mathrm{MNP})}_{\mathrm{sem}}(\tau_{ss})/P^{(0)}_{\mathrm{sem}}(\tau_{ss}). \tag{32}$$

3. Results and discussions

We locate the center of mass of the dye molecule at $(x,y,z)_{\mathrm{mol}} = (0,0,0.5)$ nm in the Cartesian coordinates and that of MNP on the diagonal of $x-y$ plane, and z_{mnp} is the sum of MNP radius and z_{mol}, so the position of MNP is $(x,y,z)_{\mathrm{MNP}} = (a,a,10.5)$ nm and we take a as 4.9, assuming the surface of TiO_2 on the $x-y$ plane. In order to calculate efficiently, we

take $N(\omega)$ and $T_e(\omega)$ as constants $\overline{N}$ and $\overline{T_e}$. Here, charge injection is assumed at the middle of the semiconductor conduction band. If we do not give any special remarks, we use the parameters in Table 1.

As a reference case, we present the electron transfer dynamics from dye molecule to semiconductor without and with MNP for different molecule semiconductor coupling $\overline{T_e}$ in Fig. 2. Panel a shows by assuming mid-band injection and short laser pulse excitation that within 40 fs almost all the electrons in the excited state of dye molecule are injected into the conduction band of semiconductor for the strong coupling case ($\overline{T_e} = 0.09$ eV). In the weak coupling case, however, the injection time is about 500 fs. Although the injection time is much longer than $\tau_{inj} = \frac{\hbar}{T_e}$, it is consistent with our former calculation [18,19]. Taking one MNP in the proximity of the molecule, the dominant effect is the enhancement of populations, both the population of the excited state of dye molecule and the population of the semiconductor conduction band. Enh amounts to more than 10^3. In the case of strong as well as of weak coupling, the presence of MNP makes the injection time longer. This is due to the strong energy exchange between MNP and molecule, which is also consistent with our former results [16].

To demonstrate the effect of excitation pulse on the injection from dye molecule to semiconductor, the electron population dynamics with different pulse durations is shown in Fig. 3. For comparison of the electron population of the molecular excited-state $P_e(t)$ and the total conduction band $P_{sem}(t)$, we present them in the same coordinates. We assume that the quantity $a_p = \tau_p E_0 = 5 \times 10^6$ fs · V/m (proportional to what is known as pulse area) is constant to make sure that the excitation energy becomes comparable. It can be found that the strong excitation with short pulse duration stimulate higher population of excited state of dye and therefore conduction band of semiconductor. With the coupling to the MNP, energy transfer from MNP leads to more occupation of excited state of molecule. And, the probability of electron injection into the semiconductor is increased. Although high intensity pulse make higher population of semiconductor, the enhancement effect is more dominant for a larger duration of the laser pulse excitation. To characterize the enhancement effect by different excitation pulse durations the relation of Enh and τ_p using the same a_p is presented in Fig. 4. It shows that the enhancement factor increases rapidly with the increase of pulse duration within 200 fs region, and then tends to converge to a stable value

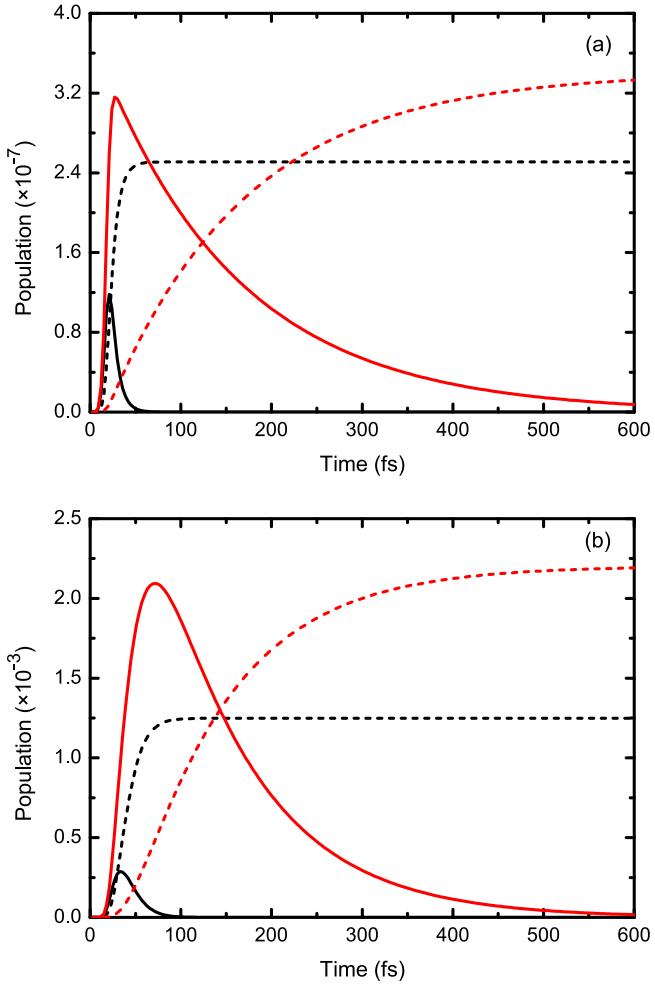

Fig. 2. Charge injection dynamics due to laser pulse excitation for weak ($\overline{T_e} = 0.02$ eV) and strong coupling ($\overline{T_e} = 0.09$ eV). Panel a: absence of the MNP, panel b: presence of the MNP. Black lines: strong coupling cases, red lines: weak coupling cases; solid lines: the excited-state population of the molecule $P_e(t)$, dashed lines: population of the total semiconductor conduction band $P_{sem}(t)$. (For interpretation of the references to colour in this figure caption, the reader is referred to the web version of this article.)

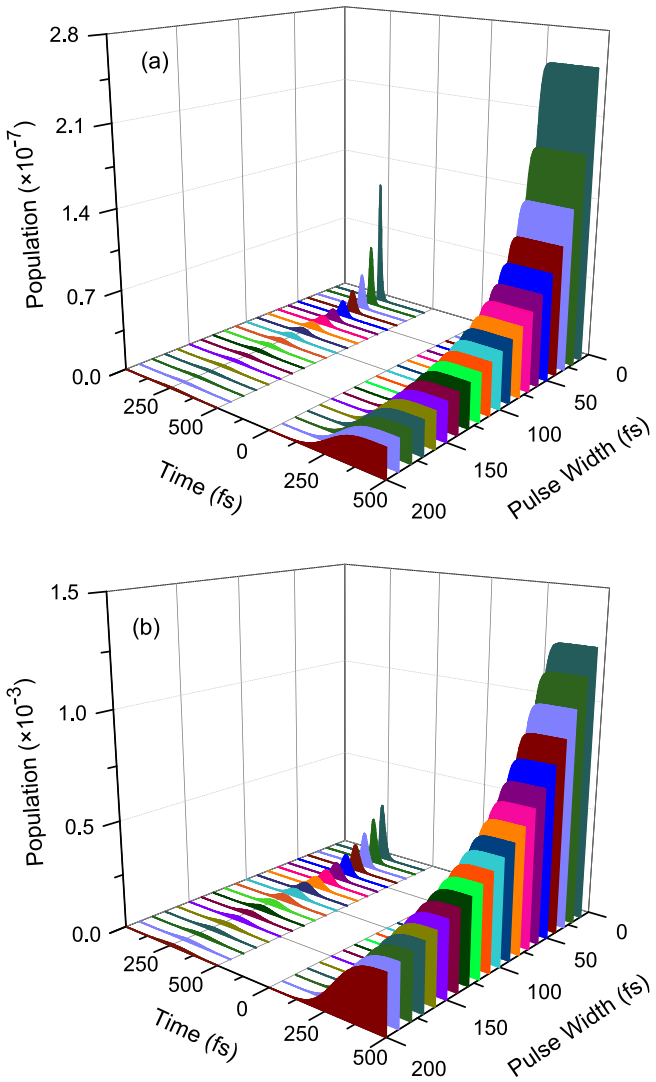

Fig. 3. Laser pulse induced charge injection dynamics for various pulse duration τ_p and intensity of field E_0 with a fixed a_p. The left lines denote the excited-state population of the molecule $P_e(t)$ and the right lines show that of the total semiconductor conduction band $P_{sem}(t)$. Panel a: absence of the MNP, panel b: presence of the MNP.

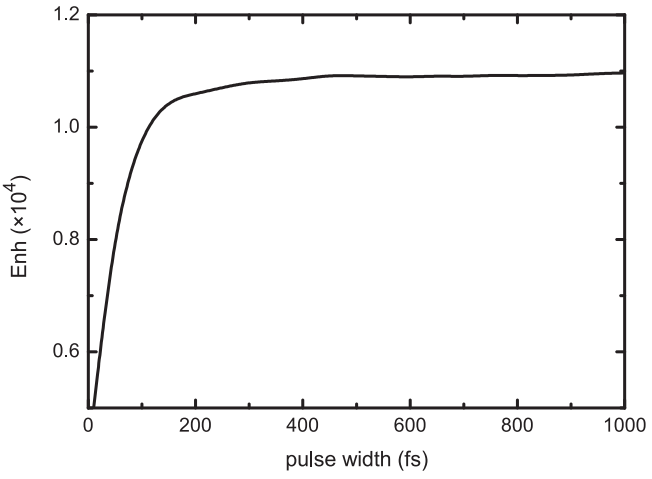

Fig. 4. Enhancement factor versus pulse duration with $a_p = 5 \times 10^6$ fs · V/m.

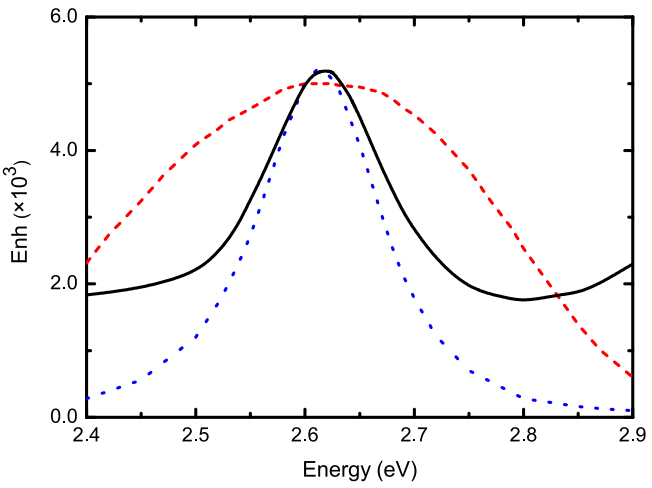

Fig. 5. Energy dependence of the enhancement factor. Black solid line: with same external field excitation energy $\hbar\omega_0 = 2.6$ eV but various excited energy of the molecule E_e, red dashed line: with same $E_e = 2.6$ eV but various $\hbar\omega_0$, blue dotted line: keeping $E_e = \hbar\omega_0$ and with various value between 2.4 eV and 2.9 eV. (For interpretation of the references to colour in this figure caption, the reader is referred to the web version of this article.)

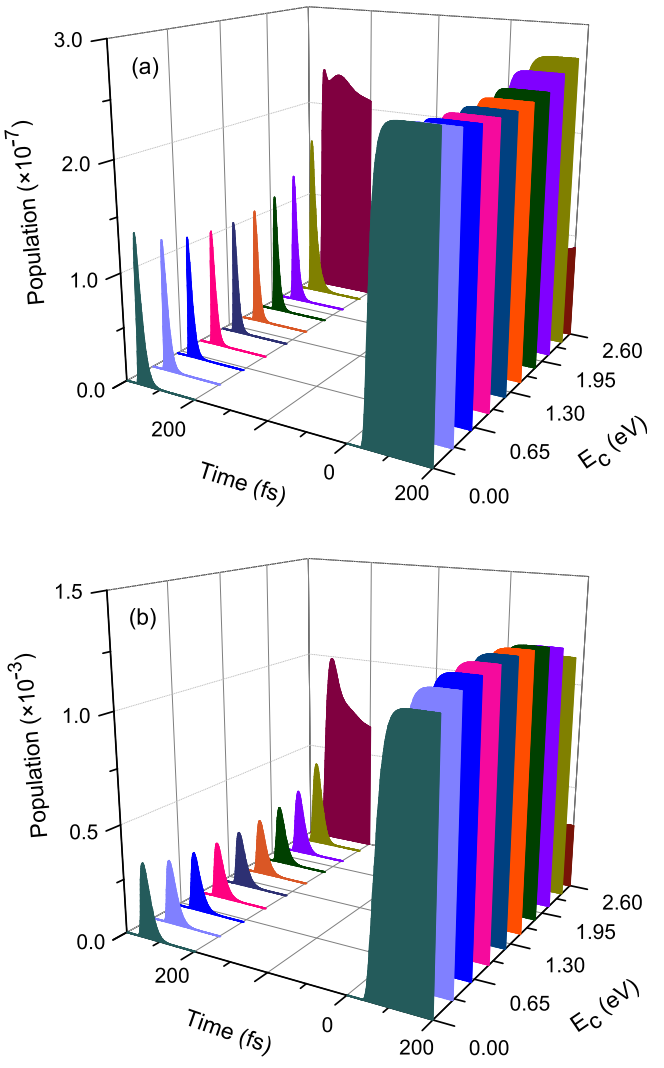

Fig. 6. Laser pulse induced charge injection dynamics, electron population versus the variety of the lower edge of the semiconductor conduction band and time. The left lines denote excited-state population of the molecule $P_e(t)$ and the right lines show the total semiconductor conduction band population $P_{sem}(t)$. Panel a: absence of the MNP, panel b: presence of the MNP.

with the variety of pulse width. It means that the enhancement factor does not rely on the intensity of pulse but on the total excitation energy when the pulse duration is larger than the injection time.

In the former calculations we assumed that the molecular excitation energy E_e is resonant to that of the MNP E_{pl}, as well as to the photon energy of external field $\hbar\omega_0$. This guarantees high enhancement efficiency. How these factors change the efficiency would be also interesting. We assume that E_e and $\hbar\omega_0$ can be changed from 2.4 eV to 2.9 eV, what is around $E_{pl} = 2.6$ eV. It is clear that the MNP enhancement on the electron population of excited state can reach its maximum when external field excitation simultaneously resonant with E_e and E_{pl}, but the enhancement on the injection seems not the case. As shown the black solid line in Fig. 5, the injection enhancement reaches its maximum with E_e at 2.62 eV, while the external field excitation energy $\hbar\omega_0$ is resonant with the plasmon energy at 2.6 eV. In a relative broad energy region, the Enh can keep a higher value with $\hbar\omega_0$ off resonant with E_e and E_{pl} (shown via the red dashed line). When E_e is more off resonant with $\hbar\omega_0 = E_{pl}$, the MNP enhancement of injection seems to

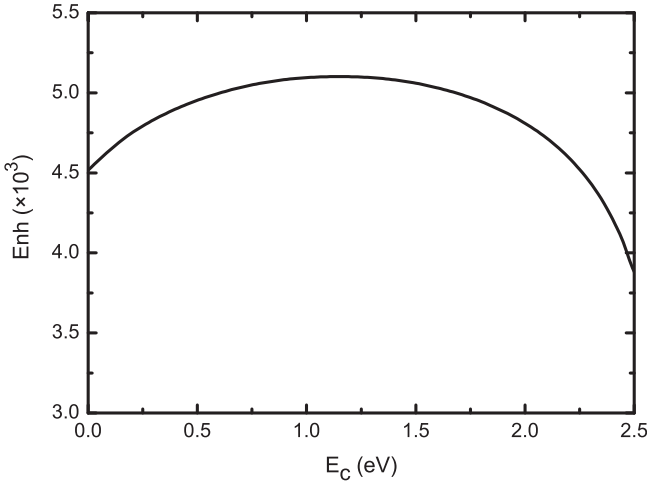

Fig. 7. Enhancement factor Enh versus the lower edge of the semiconductor conduction band E_c.

be more efficient (shown by the black solid line). If we keep $E_e = \hbar\omega_0$, the MNP enhancement of electron injection is smaller (shown by the blue dotted line). Of course, the energy region for the optimal Enh might change for different configuration of the whole system, but it provides some chances of using different dye molecule or external field to make the injection efficient.

To investigate the effect of the position of the molecular excitation energy to the conduction band, we artificially move the lower edge of the conduction band E_c to the dye molecule excitation energy. As indicated in Fig. 6, the population of the molecular excited state and the semiconductor seems similar in the region of 0–2.0 eV of band edge. When the molecular excited state is nearly resonant with the band edge, where the molecular excitation energy E_e coincides with the energy to remove the electron from the molecule and put it into the lowest TiO_2 conduction band state, the injection is blocked strongly, so higher population of molecular excited state and lower population of semiconductor conduction band can be observed. In the case where the MNP is involved, the enhancement effect is effective while the overall dynamic behavior is not change too much. As shown in Fig. 7, the most efficient region of the band edge is around 0–2.0 eV. With the further increase of the band edge, the enhancement factor decrease. To guarantee the efficient injection, the mid-band or above-band injection would be suggested.

4. Conclusion

Using the continuous energy band model for a semiconductor, charge injection dynamics from a dye molecule which is coupled to a MNP into a semiconductor conduction band is simulated. With this model, the boundary reflection of the injected electron wave function can be avoided which appears if a finite cluster model is used for the semiconductor. Accordingly, the injection enhancement due to the MNP has been calculated for a large scale semiconductor. With a MNP close to the dye molecule, the enhancement factor can reach values larger than 10^3. This is valid either for strong or weak dye-semiconductor electron transfer coupling. The excitation by an external field has been described with a fixed pulse area coefficient $a_p = \tau_p E_0$. Increasing the pulse duration τ_p the enhancement factor increases for short pulses and gets stable for long pulses. Our computations also demonstrate that in the energy region of 1 eV around the mid-band injection position, the enhancement factor is relatively stable. To get an optimal enhancement for a given position of the MNP, the relationship of E_e, E_{pl} and $\hbar\omega_0$ are also analyzed. These findings would be helpful to increase the efficiency of charge injection from a dye molecule into semiconductor and would give references for the corresponding applications.

Acknowledgements

This work has been supported by the National Natural Science Foundation of China (Grant No. 11174029).

References

[1] Lei Zhang, Jacqueline M. Cole, Anchoring groups for dye-sensitized solar cells, ACS Appl. Mater. Interfaces 7 (2015) 3427–3455.
[2] Gregory V. Hartland, Spectroscopy, imaging and solar energy conversion with plasmons, J. Phys. Chem. Lett. 3 (2012) 1421.
[3] Hanning Chen, Martin G. Blaber, Stacey D. Standridge, Erica J. DeMarco, Joseph T. Hupp, Mark A. Ratner, George C. Schatz, Computational modeling of plasmon-enhanced light absorption in a multicomponent dye sensitized solar cell, J. Phys. Chem. C 116 (2012) 10215–10221.
[4] T. Suteewong, H. Sai, R. Cohen, S. Wang, M. Bradbury, B. Baird, S.M. Gruner, U. Wiesner, Highly aminated mesoporous silica nanoparticles with cubic pore structure, J. Am. Chem. Soc. 133 (2011) 172–175.
[5] Guian Li, Xiu Li, Jianping Song, Farong Li, Shaohua Ma, Yurong Zhang, Xiaoling Fang, Preparation and fluorescence properties of co-doped nanocomposite film based on supra molecular structure, Chin. J. Chem. Phys. 19 (2006) 183–186.
[6] Carl Hagglund, S. Peter Apell, Plasmonic near-field absorbers for ultrathin solar cells, J. Phys. Chem. Lett. 3 (2012) 1275–1285.
[7] S. Mubeen, G. Hernandez-Sosa, D. Moses, J. Lee, M. Moskovits, Plasmonic photosensitization of a wide band gap semiconductor: converting plasmons to charge carriers, Nano Lett. 11 (2011) 5548–5552.
[8] M.D. Brown, T. Suteewong, R.S.S. Kumar, V. Dinnocenzo, A. Petrozza, M.M. Lee, U. Wiesner, H.J. Snaith, Plasmonic dye-sensitized solar cells using core-shell metal-insulator nanoparticles, Nano Lett. 11 (2011) 438–445.
[9] Saji Thomas Kochuveedu, Dong-Pyo Kim, Dong Ha Kim, Surface-plasmon-induced visible light photocatalytic activity of TiO_2 nanospheres decorated by Au nanoparticles with controlled configuration, J. Phys. Chem. C 116 (2012) 2500–2506.
[10] Jun Yang, Jingbi You, Chun-Chao Chen, Wan-Ching Hsu, Hai-ren Tan, Xing Wang Zhang, Ziruo Hong, Yang Yang, Plasmonic polymer tandem solar cell, ACS Nano. 5 (2011) 6210–6217.
[11] Linfang Qiao, Dan Wang, Lijian Zuo, Yuqian Ye, Jun Qian, Hongzheng Chen, Sailing He, Localized surface plasmon resonance enhanced organic solar cell with gold nanospheres, Appl. Energy 88 (2011) 848–852.
[12] Luyao Lu, Zhiqiang Luo, Tao Xu, Luping Yu, Cooperative plasmonic effect of Ag and Au nanoparticles on enhancing performance of polymer solar cells, Nano Lett. 13 (2013) 59–64.
[13] C.W. Cheng, E.J. Sie, B. Liu, C.H.A. Huan, T.C. Sum, H.D. Sun, H.J. Fan, Surface plasmon enhanced band edge luminescence of ZnO nanorods by capping Au nanoparticles, Appl. Phys. Lett. 96 (2010) 071107.
[14] Trilok Singh, D.K. Pandya, R. Singh, Surface plasmon enhanced bandgap emission of electrochemically grown ZnO nanorods using Au nanoparticles, Thin Solid Films 520 (2012) 4646–4649.
[15] Phuoc Long Truon, Xingyi Ma, Sang Jun Sim, Resonant Rayleigh light scattering of single Au nanoparticles with different sizes and shapes, Nanoscale 6 (2014) 2307–2315.
[16] Luxia Wang, Volkhard May, Plasmon enhanced heterogeneous electron transfer: a model study, J. Phys. Chem. C 118 (2014) 2812–2819.
[17] Luxia Wang, Volkhard May, Theory of plasmon enhanced interfacial electron transfer, J. Phys.: Condens. Matter 27 (2015) 134209 (9pp).
[18] Luxia Wang, Volkhard May, Laser pulse control of ultrafast heterogeneous electron transfer: a computational study, J. Chem. Phys. 121 (2004) 8039–8049.
[19] Luxia Wang, Frank Willig, Volkhard May, Theory of ultrafast photoinduced heterogeneous electron transfer, Mol. Simul. 14 (2006) 1–17.
[20] S. Ramakrishna, Matthew Pelton, Stephen K. Gray, Tamar Seideman, Theory of ultrafast photoinduced heterogeneous electron transfer, J. Phys. Chem. C 119 (2015) 22640–22645.
[21] E.R. Encina, E.A. Coronado, Plasmon coupling in silver nanosphere pairs, J. Phys. Chem. C 114 (2010) 3918–3923.
[22] I. Zelinskyi, Y. Zhang, V. May, Supramolecular complex coupled to a metal nanoparticle: computational studies on the optical absorption, J. Phys. Chem. A 116 (2012) 11330–11340.